

# A Soft Interaction Model at Ultra High Energies: Amplitudes, Cross Sections and Survival Probabilities

---

**E. Gotsman\***, **E. Levin<sup>†</sup>** and **U. Maor<sup>‡</sup>**

*Department of Particle Physics, School of Physics and Astronomy  
Raymond and Beverly Sackler Faculty of Exact Science  
Tel Aviv University, Tel Aviv, 69978, Israel*

**ABSTRACT:** In this paper we present a two channel model with the goal of reproducing the soft scattering data available in the ISR-Tevatron energy range, and extend the model results to LHC and Cosmic Rays energies. A characteristic feature of the model is that we represent the sum of all diffractive final states at a vertex, by a single diffractive state. Our two main results are: (i) The approach of the elastic scattering amplitude to the black disc bound is very slow, reaching it at energies far higher than the GZK ankle cutoff. (ii) Our predicted survival probability for Higgs exclusive central diffractive production at the LHC is 0.7%, which is considerably smaller than our previous estimate. The above features are compatible with a parton-like model in which the traditional soft Pomeron is replaced by an amplitude describing the partonic system, which is saturated in the soft (long distance) limit.

**KEYWORDS:** Soft Pomeron, Hard Pomeron, Diffractive Cross Sections, Survival Probability, Unitarity, Black disc bound.

*PACS: 13.85.-t, 13.85.Hd, 11.55.-m, 11.55.Bq*

---

\*Email: gotsman@post.tau.ac.il.

<sup>†</sup>Email: leving@post.tau.ac.il, levin@mail.desy.de.

<sup>‡</sup>Email: maor@post.tau.ac.il.

---

## Contents

<b>1. Introduction</b>	<b>1</b>
<b>2. The GLM Model</b>	<b>3</b>
2.1 Single channel model	3
2.2 Two channel model	4
<b>3. Fit to the ISR-Tevatron Experimental Data</b>	<b>6</b>
3.1 Model A	6
3.2 Model B	7
3.3 Results	7
<b>4. Predictions for LHC and Cosmic Ray Energies</b>	<b>9</b>
<b>5. Survival probabilities in the GLM model</b>	<b>11</b>
<b>6. The Role of Unitarity at High Energies</b>	<b>14</b>
6.1 Unitarity experimental signatures	14
6.2 An amplitude analysis of unitarity at very high energies	14
<b>7. Conclusions</b>	<b>18</b>

---

## 1. Introduction

The GLM model is based on a two channel eikonal like solution of the  $s$ -channel unitarity equation [1]. Our present investigation is based on an improved model, and we calculate and discuss its predictions and implications at the LHC and Cosmic Rays energies. For the correct degrees of freedom, the partial amplitude for scattering of state ‘ $i$ ’ with state ‘ $k$ ’ can be written as

$$A_{i,k}^{i',k'}(s,b) = i \delta_{i,i'} \delta_{k,k'} \left( 1 - \exp \left( -\frac{\Omega_{i,k}(s,b)}{2} \right) \right). \quad (1.1)$$

$i$  and  $k$  represent sets of quantum numbers which diagonalize the interaction matrix. The opacities  $\Omega_{i,k}$  are arbitrary real functions of energy and impact parameter.

As long as  $\Omega_{i,k}$  are not explicitly specified, our presentation is model independent. We assume that the scattering amplitude at high energies is predominantly imaginary. In our original single channel model [2] we assumed that the opacity is determined by the exchange of a soft Pomeron represented by a factorized fixed pole in the complex angular momentum ( $J$ ) plane. This simplified assumption is not maintained in the present, more elaborate two channel model, where factorization of the coupling constants is relaxed. These features are compatible with our present partonic picture, where the soft Pomeron, is replaced by the soft distance limit, of the amplitude for a saturated partonic system [3]. This approach is supported by eikonal-like models [4,5], which reproduce the e-p DIS data over a wide range of  $Q^2$ , starting from very small virtualities. Details of our parametrization are presented in Sec. 2.

We shall elaborate on the following issues:

- 1) Our original investigation [1] neglected the double diffraction state. Experimental data on this channel is now available [6] and it makes the simplified two amplitude approximation doubtful. The present three amplitude analysis is based on an updated data base which includes the published  $p$ - $p$  and  $\bar{p}$ - $p$  data points of  $\sigma_{tot}$ , the integrated values of  $\sigma_{el}$ ,  $\sigma_{sd}$ ,  $\sigma_{dd}$  and the forward elastic slope  $B_{el}$  in the ISR-Tevatron energy range. The forward slopes of the SD and DD final states, as well as  $\rho = \frac{Re a_{el}(t=0,s)}{Im a_{el}(t=0,s)}$ , are predictions of the model.
- 2) Based on this initial investigation, our present analysis aims at providing reliable predictions of the quantities to be measured at 14  $TeV$ , the LHC c.m. energy. Our output also covers the broad Cosmic Ray energy range up to the GZK limit. We validate the consistency of our calculations with unitarity by extending our output up to the Planck mass.
- 3) One requires a reliable formulation of soft scattering to calculate the survival probability of large rapidity gaps (LRG), initiated by the underlying soft rescatterings of the spectator partons, in an inelastic diffractive (soft or hard) process [2, 7, 8]. This calculation is of particular importance for the assessment of the discovery potential for LHC Higgs production in an exclusive central diffractive process. This channel, with a clean two LRG signature, has a relatively good signal to background ratio. The extraction of a clear diffractive Higgs signal at the LHC, requires a precise knowledge of the cross section and transverse momentum behavior of the single diffractive production channel, which provides a significant contribution to the background of interest. We shall investigate the SD channel in some detail.
- 4) Some of the fundamental consequences of s-channel unitarity in the high energy limit are not clear as yet. We wish to assess the rate that the elastic scattering amplitude reaches the unitarity black disc bound in  $b$ -space. This is, obviously, coupled to the behavior of the corresponding diffractive amplitudes. A related piece of information, which is still unknown, is the rate at which the proton black core expands with energy in  $b$ -space. At present, different models provide drastically different assessment of this phenomenon. Our advantage of having a specific model enables us to study in detail the behavior of the amplitudes as functions of energy and impact parameter, and, consequently, we are able to provide a numerical description of the process. Our approach differs from alternative treatments which are based on general assessments which are not accompanied by a detailed analysis of the soft scattering data. See, for example Ref. [9].

The organization of this paper is as follows: In Sec.2 we briefly summarize the general properties of the eikonal approach and formulate our model. Following, we review the extension from GLM single channel to two channels. In Sec.3 we present the three models we have considered and the output of our calculations in the ISR-Tevatron energy range. Sec.4 is devoted to a presentation of our predictions for LHC and Cosmic Ray energies. In Sec.5 we discuss survival probability calculations in the GLM models applied to Higgs production at LHC. Sec.6 is devoted to a detailed analysis of the onset of unitarity effects at exceedingly high energies, and the approach to the black disc bound in  $b$ -space. Our conclusions are presented in Sec.7.

## 2. The GLM Model

### 2.1 Single channel model

The main assumption of the single channel GLM model is that hadrons are the correct degrees of freedom at high energy, diagonalizing the scattering matrix. This model [2] fits  $\sigma_{tot}$ ,  $\sigma_{el}$  and  $B_{el}$  well, but fails to reproduce the inelastic diffractive final states. This is evident in the relatively better measured SD channel, in which the calculated normalization and energy dependence of  $\sigma_{sd}$  fail to agree with the experimental data [2]. This is not surprising as the input assumption of this class of models, that  $\frac{\sigma_{sd}}{\sigma_{el}}$  is negligibly small, is not compatible with the data [10].

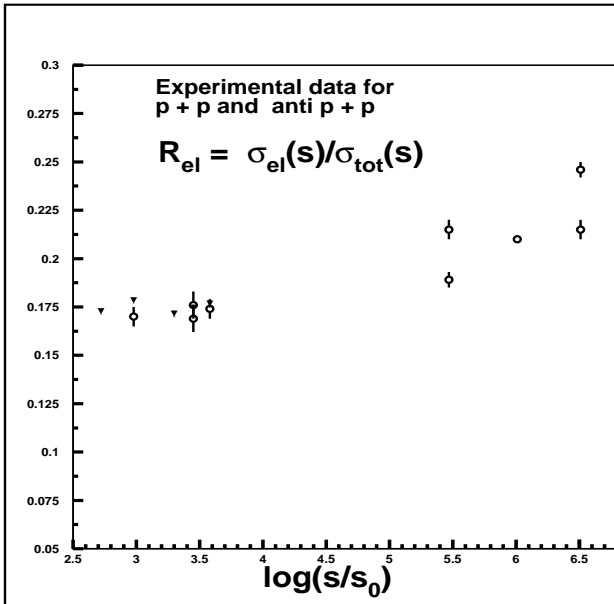


Figure 1: Energy dependence of  $R_{el}$ .

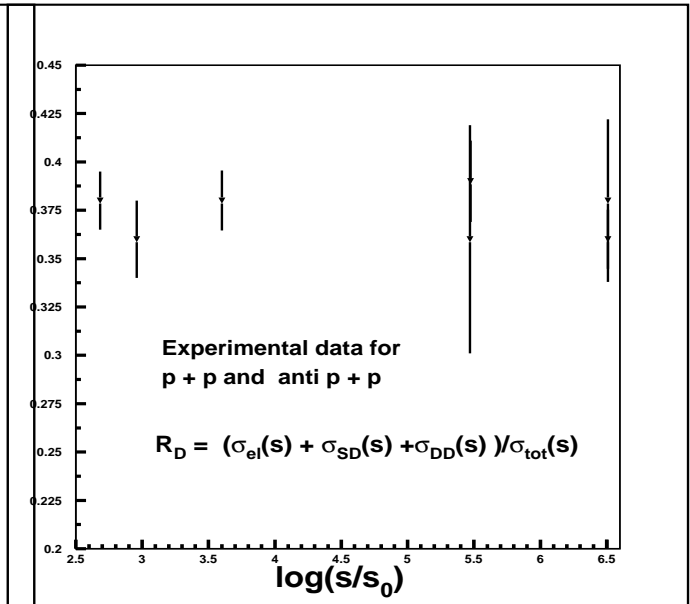


Figure 2: Energy dependence of  $R_D$ .

It is instructive to see the ISR-Tevatron experimental data presented in Fig. 1 and Fig. 2. Fig. 1 shows the power like increase of the ratio  $R_{el} = \frac{\sigma_{el}}{\sigma_{tot}}$  with  $s$ , which is compatible with our parametrization (soft Pomeron like), and can be reproduced in a single channel eikonal model in the ISR-LHC energy range [11].

Defining  $\sigma_{diff} = \sigma_{sd} + \sigma_{dd}$ , the ratio  $R_D = \frac{\sigma_{el} + \sigma_{diff}}{\sigma_{tot}}$ , which is shown in Fig. 2, behaves approximately as a constant of about 0.37-0.38. This is incompatible with the assumed exchange of an unscreened soft Pomeron, where,  $R_{el}$  and  $R_D$  are expected to have approximately the same energy dependence. In a single channel eikonal model  $\frac{\sigma_{diff}}{\sigma_{el}}$  is a small parameter. i.e., diffractive scattering is treated as a perturbative effect. As such, this ratio tends to a small constant at low energies, and approaches zero in the high energy limit. This behavior is in contradiction with the experimental data shown in Fig. 2.

In the following we show that the deficiencies of the single channel eikonal model are eliminated in a more elaborate two channel model in which diffractive, alongside elastic, scatterings are included in the rescattering chain.

## 2.2 Two channel model

The GLM two channel model has been described in our previous publications (see Refs. [1, 12–14] and references therein). In this formalism, diffractively produced hadrons at a given vertex are considered as a single hadronic state described by the wave function  $\Psi_D$ , which is orthonormal to the wave function  $\Psi_h$  of the incoming hadron (proton in the case of interest),  $\langle \Psi_h | \Psi_D \rangle = 0$ . We introduce two wave functions  $\Psi_1$  and  $\Psi_2$  that diagonalize the 2x2 interaction matrix  $\mathbf{T}$

$$A_{i,k}^{i',k'} = \langle \Psi_i | \Psi_k | \mathbf{T} | \Psi_{i'} | \Psi_{k'} \rangle = A_{i,k} \delta_{i,i'} \delta_{k,k'}, \quad (2.1)$$

In this representation the observed states are written in the form

$$\Psi_h = \alpha \Psi_1 + \beta \Psi_2, \quad (2.2)$$

$$\Psi_D = -\beta \Psi_1 + \alpha \Psi_2, \quad (2.3)$$

where,  $\alpha^2 + \beta^2 = 1$ .

Using Eq. (2.1) we can rewrite the unitarity equations in the form

$$Im A_{i,k}(s, b) = |A_{i,k}(s, b)|^2 + G_{i,k}^{in}(s, b), \quad (2.4)$$

where  $G_{i,k}^{in}$  is the contribution of all non diffractive inelastic processes. i.e., it is the summed probability for these final states to be produced in the scattering of particle  $i$  off particle  $k$ . The simple solution to Eq. (2.4) has the same structure as in the single channel formalism,

$$A_{i,k}(s, b) = i \left( 1 - \exp \left( -\frac{\Omega_{i,k}(s, b)}{2} \right) \right), \quad (2.5)$$

$$G_{i,k}^{in}(s, b) = 1 - \exp(-\Omega_{i,k}(s, b)). \quad (2.6)$$

From Eq. (2.6) we deduce the probability that the initial projectiles ( $i, k$ ) reach the final state interaction unchanged, regardless of the initial state rescatterings, is given by  $P_{i,k}^S = \exp(-\Omega_{i,k}(s, b))$ .

Our presentation, thus far, is model independent. Model dependent parameters are introduced so as to obtain explicit expressions for the opacities  $\Omega_{i,k}(s, b)$ . As stated in the Introduction, we now replace the

simple Pomeron J-pole dynamic input, by an updated interpretation, in which the Pomeron is replaced by the description of a partonic system, which goes through a process of saturation when approaching the soft, large distance limit [3]. This point of view is compatible with eikonal type models which reproduce DIS e-p scattering data over the whole  $Q^2$  range, i.e. from low to high photon virtualities [4, 5].

Even though we now suggest a more elaborate partonic description for the dynamics of interest, we still maintain a simple form for the opacities  $\Omega_{i,k}$ ,

$$\Omega_{i,k}(s, b) = \nu_{i,k}(s) \Gamma(s, b). \quad (2.7)$$

In the above

$$\nu_{i,k}(s) = \sigma_{i,k}^0 \left( \frac{s}{s_0} \right)^\Delta, \quad (2.8)$$

and

$$\Gamma_{i,k}(s, b) = \frac{1}{\pi R_{i,k}^2(s)} \exp\left(-\frac{b^2}{R_{i,k}^2(s)}\right). \quad (2.9)$$

The energy term  $\nu_{i,k}$  is a power in  $s$  reflecting a long standing observation [15] that the cross section of DIS collisions behaves, at least approximately, as a power in energy. The b-profile  $\Gamma_{i,k}(s, b)$  are assumed to be Gaussians. Since the t-space transform of a Gaussian in impact parameter is proportional to  $\exp\left(-\frac{R_{i,k}^2}{4}|t|\right)$ , our parametrization provides a very good reproduction of the small  $|t|$  elastic forward cone data, covering more than 95% of the elastic scattering events. A general property of a b-Gaussian profile is that the small  $t$  region transforms to high  $b$ , and high  $t$  to small  $b$ . The structure of our opacities, as presented in Eq. (2.7), has the advantage that it is general enough to serve as a parametrization of wide class of dynamical models. It is applicable both to a conventional soft Pomeron exchange, as well as a hard Pomeron process such as  $\gamma + p \rightarrow J/\Psi + p$  [16].

Even though we now suggest a more elaborate partonic description for the dynamics of interest, we still choose for our radius a Regge-like expression

$$R_{i,k}^2(s) = R_{0,i}^2 + R_{0,k}^2 + 4\alpha' \ln(s/s_0), = R_{0;i,k}^2 + 4\alpha' \ln\left(\frac{s}{s_0}\right) \quad (2.10)$$

in which  $R_{0,j}^2$  and  $\alpha'$  are fitted parameters. Indeed, the fitted values of  $\alpha'$  corresponding to Models B(1) and B(2), to be discussed in the next Section, differ from the values typical to Regge phenomenology. Note that  $R_{0,2}^2 = 0$ .

In general, we have to consider four possible re-scattering processes. For the case of  $p$ - $p$  (or  $\bar{p}$ - $p$ ) the two quasi-elastic amplitudes are equal  $a_{1,2} = a_{2,1}$ , and we thus have three rescattering amplitudes: elastic, SD and DD. These amplitudes are presented in the two channel formalism in the following form [1, 12, 14]

$$a_{el}(s, b) = i\{\alpha^4 A_{1,1} + 2\alpha^2 \beta^2 A_{1,2} + \beta^4 A_{2,2}\}, \quad (2.11)$$

$$a_{sd}(s, b) = i\alpha\beta\{-\alpha^2 A_{1,1} + (\alpha^2 - \beta^2)A_{1,2} + \beta^2 A_{2,2}\}, \quad (2.12)$$

$$a_{dd} = i\alpha^2 \beta^2 \{A_{1,1} - 2A_{1,2} + A_{2,2}\}. \quad (2.13)$$

It should be stressed that in this approach diffraction dissociation appears as an outcome of the elastic scattering of  $\Psi_1$  and  $\Psi_2$ , the correct degrees of freedom of our model.

The corresponding cross sections are given by

$$\sigma_{tot}(s) = 2 \int d^2b \text{Im} a_{el}(s, b), \quad (2.14)$$

$$\sigma_{el}(s) = \int d^2b |a_{el}(s, b)|^2, \quad (2.15)$$

$$\sigma_{sd}(s) = \int d^2b |a_{sd}(s, b)|^2, \quad (2.16)$$

$$\sigma_{dd}(s) = \int d^2b |a_{dd}(s, b)|^2. \quad (2.17)$$

In a simplified version we considered a two amplitude model, where  $a_{dd}$  is assumed to be small enough to be neglected implying that  $A_{2,2} = 2A_{1,2} - A_{1,1}$ . In this model [1] only elastic and SD rescatterings are included in the eikonal screening correction. In our past publications we referred to the GLM eikonal models according to the number of the rescattering channels considered, i.e. elastic [2], elastic+SD [1] and elastic+SD+DD [12]. In retrospect, we consider it more appropriate to define these models according to the dimensionality of their amplitude base. We, therefore, call the 2x2 configuration a two channel model, making the distinction between its two and three amplitude representations.

### 3. Fit to the ISR-Tevatron Experimental Data

We have studied three models, with different parameterization of  $\Omega_{i,k}$ , which were compared with the global experimental data base. The models are based on the general formulae given in Eq. (2.5) - Eq. (2.10), with different input assumptions. Note that the fit has, in addition to the contribution in the form of Eq. (2.7), also a secondary Regge sector (see Ref. [1, 2]). This is necessary as the data base contains many experimental points from lower ISR energies. A study of the vacuum component alone, without a Regge contribution, is not possible at this time, since the corresponding high energy sector of the available data base is too small to constrain the fitted parameters of Eq. (2.7). Unlike the assumed Pomeron exchange in the vacuum channel, the existence of the secondary Regge trajectories is well established both theoretically and experimentally. As the goal of this paper is to obtain predictions in the LHC and Cosmic Rays energy range, where the contribution of the secondary Regge trajectories is negligibly small, the Regge parameters are not quoted in this paper, and will be given in a separate publication. Note that at the Tevatron the Regge sector contribution is less than 1%.

#### 3.1 Model A

Model A is a two amplitude model, which was considered in Ref. [1] in detail. Its main assumption is that the double diffraction cross section is small enough to be omitted from the fitted data base. As we saw,

this allows us to express  $\Omega_{2,2}$  in terms of  $\Omega_{1,1}$  and  $\Omega_{1,2}$ , as such, this model breaks Regge factorization. We obtain (see Refs. [1,14])

$$a_{el}(s, b) = i \left( 1 - \exp \left( -\frac{\Omega_{1,1}(s, b)}{2} \right) - 2\beta^2 \exp \left( -\frac{\Omega_{1,1}(s, b)}{2} \right) \left( 1 - \exp \left( -\frac{\Delta\Omega(s, b)}{2} \right) \right) \right), \quad (3.1)$$

$$a_{sd}(s, b) = -i\alpha\beta \exp \left( -\frac{\Delta\Omega(s, b)}{2} \right) \left( 1 - \exp \left( -\frac{\Delta\Omega(s, b)}{2} \right) \right), \quad (3.2)$$

where,  $\Delta\Omega = \Omega_{1,2} - \Omega_{1,1}$ . Following Ref. [1], we assume both  $\Omega_{1,1}$  and  $\Delta\Omega$  to be Gaussians in  $b$ .

$$\Omega_{1,1}(s, b) = \frac{\sigma_{1,1}^0}{\pi R_{1,1}^2(s)} \left( \frac{s}{s_0} \right)^\Delta \exp \left( -\frac{b^2}{R_{1,1}^2(s)} \right), \quad (3.3)$$

$$\Delta\Omega(s, b) = \frac{\sigma_\Delta^0}{\pi R_\Delta^2(s)} \left( \frac{s}{s_0} \right)^\Delta \exp \left( -\frac{b^2}{R_\Delta^2(s)} \right). \quad (3.4)$$

Note that in this two amplitude model  $R_\Delta^2 = \frac{1}{2}R_{0;11}^2 + 4\alpha' \ln(s/s_0)$  is the radius of  $\Delta\Omega(s, b)$ . We have also studied a two amplitude model in which both  $\Omega_{1,1}$  and  $\Omega_{1,2}$  are Gaussians in  $b$ . The output obtained in this two amplitude model is compatible with Model A. This is not surprising as  $\sigma_\Delta^0 \gg \sigma_{1,1}^0$  (see Table 1).

### 3.2 Model B

In the three amplitude model we do not make any assumptions regarding the values of the double diffraction cross sections [6] which are contained in our fitted data base. We use the formulae of Eq. (2.7) and Eq. (2.10) to parameterize the three opacities  $\Omega_{1,1}$ ,  $\Omega_{1,2}$  and  $\Omega_{2,2}$ , which are taken to be Gaussians in  $b$ . If we assume the soft Pomeron to be a simple fixed J pole the knowledge of two out of those three opacities determines the third. We denote this option Model B(1). In this model  $\sigma_{1,2}^0 = \sqrt{\sigma_{1,1}^0 \times \sigma_{2,2}^0}$ . As we shall see, the fit corresponding to Model B(1) is not satisfactory. We have, also, studied Model B(2) in which a factorization of  $\sigma_{i,k}^0$  is not assumed. Accordingly,  $\sigma_{1,1}^0$ ,  $\sigma_{1,2}^0$  and  $\sigma_{2,2}^0$  are independent fitted parameters of the model. This model reflects our approach to the soft interaction as the continuation of the hard processes in the saturated soft region. We would like to stress, that this model gives a very good reproduction of the data.

### 3.3 Results

The parameters of Model A are based on a fit to a 55 experimental data points base which includes the  $p$ - $p$  and  $\bar{p}$ - $p$  total cross sections, integrated elastic cross sections, integrated single diffraction cross sections, and the forward slope of the elastic cross section in the ISR-Tevatron energy range. We did not include the Cosmic Ray air showers estimated total cross sections in our data base, as they require additional model dependent assumptions [17]. As stated, we neglected the reported DD cross section points. The fitted parameters of Model A are listed in Table 1 with a corresponding  $\chi^2/(d.o.f)$  of 1.50.

Model	$\Delta$	$\beta$	$R_{0;1,1}^2$	$\alpha'_P$	$\sigma_{1,1}^0$	$\sigma_{2,2}^0$	$\sigma_{\Delta}^0$	$\sigma_{1,2}^0$
A	0.126	0.464	$16.34 \text{ GeV}^{-2}$	$0.200 \text{ GeV}^{-2}$	$12.99 \text{ GeV}^{-2}$	N/A	$145.6 \text{ GeV}^{-2}$	N/A
B(1)	0.150	0.526	$20.80 \text{ GeV}^{-2}$	$0.184 \text{ GeV}^{-2}$	$4.84 \text{ GeV}^{-2}$	$4006.9 \text{ GeV}^{-2}$	N/A	$139.3 \text{ GeV}^{-2}$
B(2)	0.150	0.776	$20.83 \text{ GeV}^{-2}$	$0.173 \text{ GeV}^{-2}$	$9.22 \text{ GeV}^{-2}$	$3503.5 \text{ GeV}^{-2}$	N/A	$6.5 \text{ GeV}^{-2}$

**Table 1:** Fitted parameters for Models A, B(1) and B(2).

The fits to Models B(1) and B(2) are based on an updated data base which includes the data base used for Model A, plus 5 double diffraction cross sections data points [6]. In Table 1 we present two sets of fitted parameters for Model B. The factorizable Model B(1) does not give a good reproduction of the data, with a  $\chi^2/(d.o.f.)=2.30$ . Part, but not all, of this large  $\chi^2$  is contributed by the DD data, where the model predictions are significantly below the experimental points. Model B(2), with a  $\chi^2/(d.o.f.) = 1.25$ , provides a very good reproduction of the data base. Its seemingly high  $\chi^2$  reflects the poor quality of the published SD data points. The model provides a very good reproduction of the DD data points.

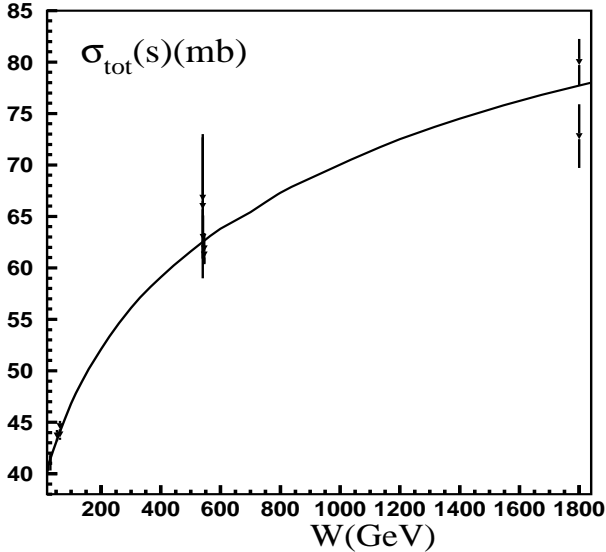


**Figure 3:** UA4-Tevatron energy dependence of  $\sigma_{tot}$  in Model B(2).

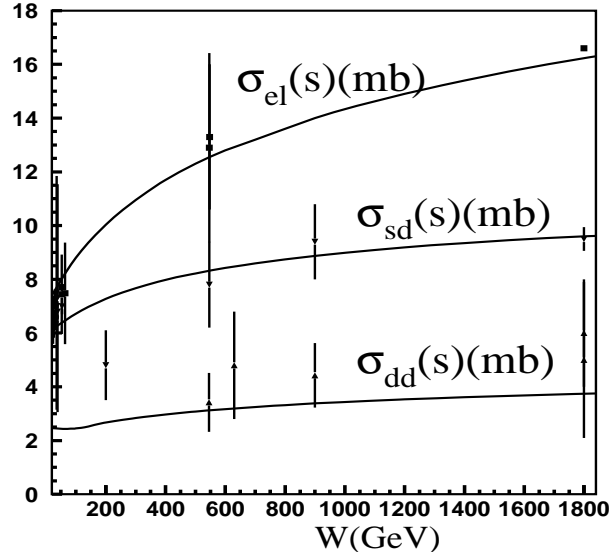


**Figure 4:** UA4-Tevatron energy dependence of  $\sigma_{el}$ ,  $\sigma_{sd}$  and  $\sigma_{dd}$  in Model B(2).

Model A and Model B(2) give compatible reproductions of our data base without the DD points. To this end, we refer to the figures of Ref. [1] and Fig. 3 and Fig. 4 of this paper. The calculations of  $B_{sd}$  and  $\rho$  were executed with the fitted parameters of Model B(2). Neglecting the Regge contribution, we reproduce the higher energy experimental data points obtained by UA4, CDF and E710.

Obviously, factorization violations in the coupling input of Model A and Model B(2) are very interesting and support our partonic saturation approach. We hope that our present results will encourage additional studies of the intriguing relations between, what are traditionally called, soft and hard Pomerons.

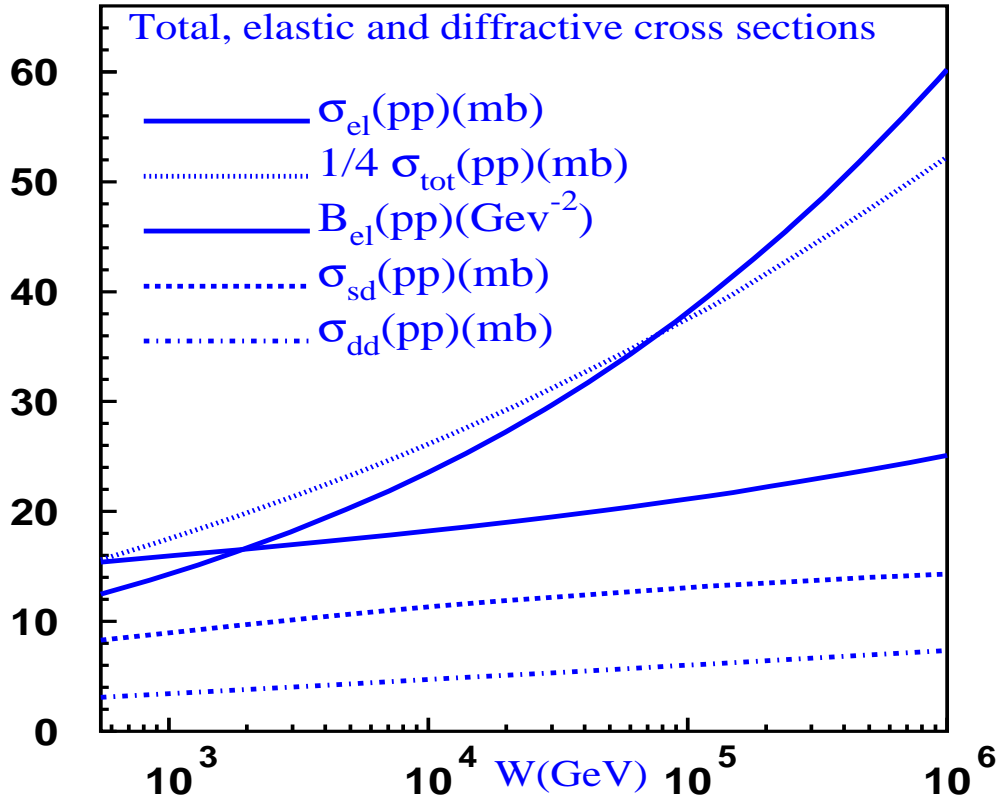
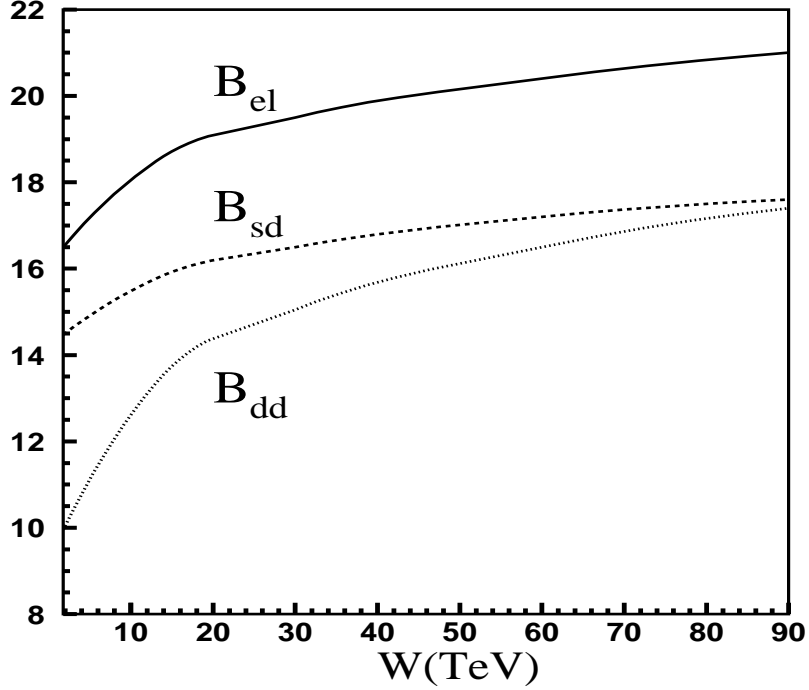


Figure 5: Total, elastic and diffractive cross sections in Model B(2).

#### 4. Predictions for LHC and Cosmic Ray Energies

Model B(2) cross section and slopes predictions for LHC and Cosmic Ray energies are summarized in Fig. 5, Fig. 6 and Table 2. At  $W=14 TeV$  (LHC energy) our predicted cross sections are:  $\sigma_{tot} = 110.5 mb$ ,  $\sigma_{el} = 25.3 mb$ ,  $\sigma_{sd} = 11.6 mb$  and  $\sigma_{dd} = 4.9 mb$ . These predictions are slightly higher than those obtained [1] in Model A. The corresponding forward slopes are:  $B_{el} = 20.5 GeV^{-2}$ ,  $B_{sd} = 15.9 GeV^{-2}$  and  $B_{dd} = 13.5 GeV^{-2}$ . One can see that the predicted cross section of the diffractive channels, as compared with the elastic cross section, is relatively large and should be considered in the estimates for the background for diffractive Higgs production process. The ratio of  $\sigma_{el}/\sigma_{tot}$  at the LHC is predicted to be less than 0.25. This is a signature that at the LHC energy the proton-proton (anti proton) elastic scattering amplitude is well below the black disc asymptotic bound. We shall elaborate on this point in Sec. 6.

Checking the predictions presented in Table 2, we note a systematic behavior of the listed cross sections from which we learn about the gross features of unitarity, spanning the energies from accelerator range to



**Figure 6:** Energy dependence of  $B_{el}$ ,  $B_{sd}$  and  $B_{dd}$  in Model B(2).

$\sqrt{s}$ TeV	$\sigma_{tot}^{DL}$ mb	$\sigma_{tot}$ mb	$\sigma_{el}$ mb	$\sigma_{sd}$ mb	$\sigma_{dd}$ mb	$B_{el}$ $GeV^{-2}$	$R_{el}$	$R_D$	$\frac{\sigma_{diff}}{\sigma_{el}}$
1.8	73.0	78.0	16.3	9.6	3.8	16.8	0.21	0.38	0.83
14	101.7	110.5	25.3	11.6	4.9	20.5	0.23	0.38	0.65
30	115.0	124.8	29.7	12.2	5.3	22.0	0.24	0.38	0.59
60	128.6	139.0	34.3	12.7	5.7	23.4	0.25	0.38	0.54
120	143.9	154.0	39.6	13.2	6.1	24.9	0.26	0.38	0.49
250	162.0	172.0	45.9	13.6	6.6	26.5	0.27	0.38	0.44
500	181.2	190.0	52.7	14.0	7.0	28.1	0.28	0.39	0.40
1000	202.7	209.0	60.2	14.3	7.4	29.8	0.29	0.39	0.10
$10^{11}$	3970.0	1070.0	451.2	21.6	19.5	109.9	0.42	0.46	0.09
$1.22 \cdot 10^{19}$ (Planck)	26400.0	1970.0	871.4	25.5	27.7	202.6	0.44	0.47	0.06

**Table 2:** Cross sections and elastic slope in Model B(2).  $\sigma_{tot}^{DL}$  is presented for comparison.

the Planck mass.

1) The difference between DL non screened total cross section predictions [15] and GLM is small up to the GZK ankle, which is a practical upper bound for Cosmic Ray energies with which we can obtain

information relevant to our study.

2) The predicted ratio of  $R_{el}$  and  $R_D$  are well below 0.5 up to GZK and above. Close to the Planck mass the ratios approach 0.5.

3) From Table 2 we see that while  $R_{el}$  grows very slowly with energy,  $R_D$  is essentially a constant, slightly less than 0.4, all through the Cosmic Ray energy range. Accordingly, the predictions for the diffractive channels, though increasingly suppressed with energy relative to the elastic channel, cannot be ignored.

4) Well above the GZK cutoff the ratio  $R_{el}$  grows more rapidly with energy while  $\sigma_{diff}/\sigma_{el}$  which is less than 0.1, diminishes slowly. At the Planck mass we see that  $R_{el}=0.44$  and  $R_D=0.47$ .

5) The above predictions suggest a very slow onset of unitarity constraints on the total and integrated cross sections with growing energy. We wish to remind the reader that in eikonal models the asymptotic behavior of  $\sigma_{tot}$ , with a logarithmic accuracy, is  $ln^2(s/s_0)$ , that of  $\sigma_{el}$  is  $\frac{1}{2}ln^2(s/s_0)$ , while that of  $\sigma_{diff}$  is only  $ln(s/s_0)$ . This issue will be discussed in detail in Sec. 6.

## 5. Survival probabilities in the GLM model

In the following we shall limit our discussion to the survival probability of Higgs production in an exclusive central diffractive process, calculated in a three amplitude model. A general review of survival probability calculations can be found in Ref. [14]. Our one and two amplitude model calculations have been published [12, 18].

In our model we assume an input Gaussian  $b$ -dependence for both the elastic opacities, specified in Eq. (2.7) - Eq. (2.10), and the similar structured hard diffractive amplitude of interest. The hard diffractive non screened cross sections in the (i,k) channel are calculated using the multi particle optical theorem [19]. As stated, they are written in the same form as the soft amplitudes

$$\Omega_{i,k}^H = \nu_{i,k}^H(s)\Gamma_{i,k}^H(b), \quad (5.1)$$

where,

$$\nu_{i,k}^H = \sigma_{i,k}^{H0} \left(\frac{s}{s_0}\right)^{\Delta_H}, \quad (5.2)$$

$$\Gamma_{i,k}^H(b) = \frac{1}{\pi R_{i,k}^2} e^{-\frac{b^2}{R_{i,k}^2}}. \quad (5.3)$$

The hard radii  $R_{i,k}^2$  are constants derived from HERA  $J/\Psi$  elastic and inelastic photo and DIS production [5, 16]. See, also, Ref. [14].

The general formulae for the calculation of the survival probability for diffractive Higgs boson production have been discussed in Refs. [12, 14, 20]. The structure of the survival probability expression is shown in Fig. 7. Accordingly,

$$\langle |S_H|^2 \rangle = \frac{N(s)}{D(s)}, \quad (5.4)$$

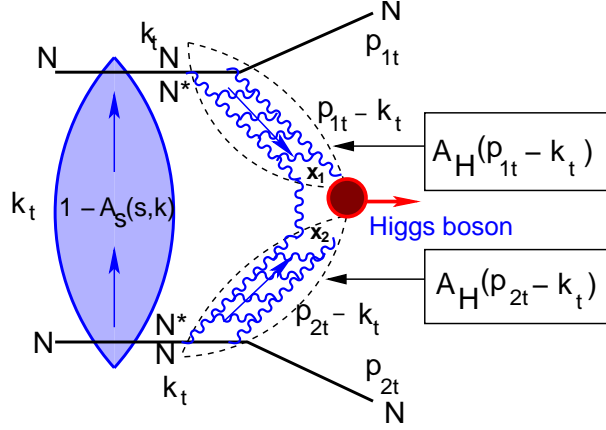


**Figure 7:** Survival probability for exclusive central diffractive production of the Higgs boson.

where,

$$N(s) = \int d^2 b_1 d^2 b_2 [A_H(s, b_1) A_H(s, b_2) (1 - A_S(s, \mathbf{b}_1 + \mathbf{b}_2))]^2, \quad (5.5)$$

$$D(s) = \int d^2 b_1 d^2 b_2 [A_H(s, b_1) A_H(s, b_2)]^2. \quad (5.6)$$

$A_s$  denotes the soft strong interaction amplitude given by Eq. (2.5). The form of  $A_H(s, b)$  has been discussed in detail in Refs. [12, 14].

Using Eq. (2.11)-Eq. (2.13), the integrands of Eq. (5.5) and Eq. (5.6) are reduced by eliminating common  $s$ -dependent expressions.

$$\begin{aligned} N(s) &= \int d^2 b_1 d^2 b_2 [A_H(s, b_1) A_H(s, b_2) (1 - A_S(\mathbf{b} = \mathbf{b}_1 + \mathbf{b}_2))]^2 \\ &= \int d^2 b_1 d^2 b_2 [(1 - a_{el}(s, b)) A_H^{pp}(b_1) A_H^{pp}(b_2) - a_{sd}(s, b) (A_H^{pd}(b_1) A_H^{pp}(b_2) + A_H^{pp}(b_1) A_H^{pd}(b_2)) \\ &\quad - a_{dd}(s, b) A_H^{pd}(b_1) A_H^{pd}(b_2)]^2, \end{aligned} \quad (5.7)$$

$$D = \int d^2 b_1 d^2 b_2 [A_H^{pp}(b_1) A_H^{pp}(b_2)]^2. \quad (5.8)$$

Following Refs. [14, 20] we introduce two hard  $b$ -profiles

$$A_H^{pp}(b) = \frac{V_{p \rightarrow p}}{2\pi B_{el}^H} \exp\left(-\frac{b^2}{2B_{el}^H}\right), \quad (5.9)$$

$$A_H^{pd}(b) = \frac{V_{p \rightarrow d}}{2\pi B_{in}^H} \exp\left(-\frac{b^2}{2B_{in}^H}\right). \quad (5.10)$$

The values  $B_{el}^H = 3.6 \text{ GeV}^{-2}$  and  $B_{in}^H = 1 \text{ GeV}^{-2}$  have been taken from the experimental HERA data on  $J/\Psi$  production in HERA (see Refs. [5, 16]).

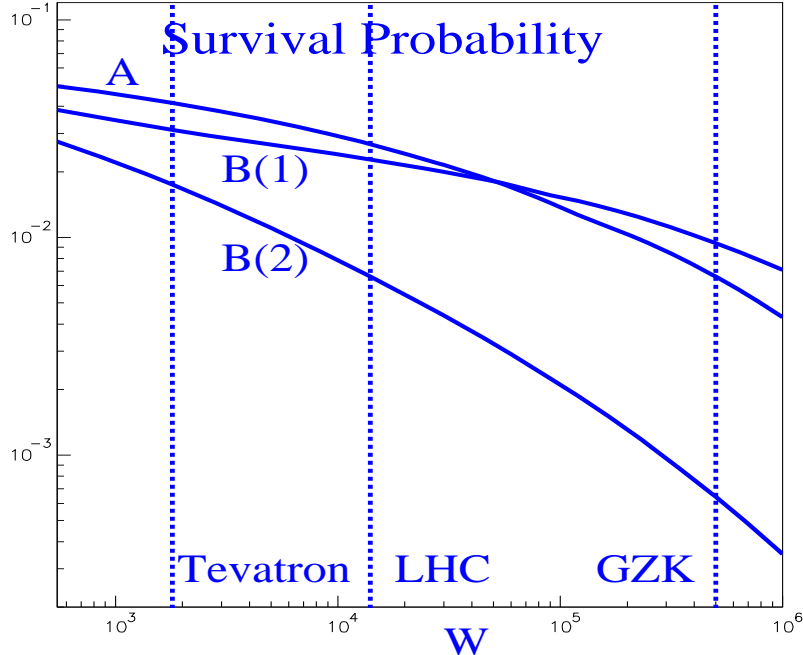


**Figure 8:** Energy dependence of centrally produced Higgs survival probability calculated in Models A, B(1), B(2).

The calculated survival probabilities have been instrumental in the theoretical interpretation of hard LRG di-jets produced at the Tevatron. For details see Ref. [14]. Using Eq. (5.4)-Eq. (5.8) we calculate the survival probability  $S_H^2$  for exclusive Higgs production in central diffraction. Our results are plotted in Fig. 8.

In the following we focus on our LHC predictions based on the above.  $S_H^2$  for exclusive Higgs production in central diffraction has been calculated [14] in the two amplitude Model A. The resulting  $S_H^2 = 0.027$  is essentially the same as the predictions of the Durham group [21] and Frankfurt et al. [9]. The main conclusion of our present results, obtained in the three amplitude B(1) and B(2) Models, is that opening more screening rescattering channels results in a reduction of the calculated value of  $S_H^2$ . Its LHC value in Model B(1) is 0.02 and in Model B(2) it is 0.007. This last result has also been obtained in Ref. [9]. Some clarifications concerning the reliability of our  $S_H^2$  estimates are in order. Our model provides an excellent reproduction of the elastic amplitude for  $b > 1.5 - 2.0 fm$ . However, since we do not reproduce  $d\sigma_{el}/dt$  outside the forward cone well [22], it would appear that our reproduction of  $a_{el}$  at small  $b$  is deficient. However, we note that a very good reproduction of  $d\sigma_{el}/dt$  at  $|t| > 0.2 GeV^2$  is obtained in eikonal models using dipoles or multi-poles in  $t$ -space for the profile function. The difference between these opacities and ours is very small at small  $b$  values [9, 11]. Accordingly, the error introduced into our calculation of  $S^2$  is

estimated to be small. An actual comparison [13] supports this conclusion.

A realistic estimate of the survival probability is crucial for the experimental discovery of a diffractive Higgs at the LHC. An educated guess of its value can be obtained, at an early stage of LHC operation, through a measurement of the rate of central hard LRG di-jets production (a GJJG configuration) coupled to a study of its expected rate in a non screened pQCD calculation.

## 6. The Role of Unitarity at High Energies

### 6.1 Unitarity experimental signatures

As it stands, the experimental support indicating the important role of unitarity considerations is confined to the energy range attained by existing accelerators. Experimental signatures associated with unitarity are observed in inelastic diffractive channels (soft and hard) at relatively low energies. This is a consequence of the unitarity suppression which, at a given impact parameter  $b$ , is given by  $P_{i,k}(s, b) = e^{-\Omega_{i,k}(s, b)}$ . After its convolution with the inelastic diffractive amplitude of interest we obtain the survival probability. In this context we identify a few significant features:

- 1) The experimental data shows a severe moderation of the energy dependence of soft diffraction at ISR energies and above, and its increase with energy is much slower than elastic scattering. This observation differs from the conventional Regge expectation in which the cross sections of elastic and inelastic diffraction are expected to have a similar energy dependence. From Table 2 we see that the ratio  $\sigma_{diff}/\sigma_{el}$  decreases monotonically with  $s$  from low energies to the Planck mass, where it is negligible. In the ISR-Tevatron range this has been observed experimentally [10], and is well reproduced by Model B(2). As we have noted our calculations at exceedingly high energy are fully compatible with the asymptotic behavior enforced by unitarity.
- 2) The predicted small value of  $S_H^2$ , the survival probability of a given LRG hard inelastic diffractive channel, has been verified in the Tevatron studies of LRG hard di-jets in various kinematical configurations. The survival probabilities are essential in order to understand both the relative smallness and energy dependence of the measured LRG hard di-jets experimental rates, when compared with pQCD estimates. Survival probabilities are essential in explaining [21] the large factorization breaking in the rates of LRG hard di-jets observed in Fermilab and HERA. The above has been systematically obtained by a few independent models, regardless of the method chosen to enforce unitarity. For details see Ref. [14].
- 3) The assessment of  $S_H^2$  is a fundamental ingredient in the experimental program to discover a Higgs boson produced in central diffraction. Its signature is that the diffractive system, observed in the  $\eta - \phi$  final state lego plot, is accompanied on both sides by a LRG. In this paper we have presented Model B(2) predicted value of  $S_H^2 = 0.007$ , smaller than our Model A prediction of  $S_H^2 = 0.027$ . Regardless of our particular formulation and estimate, unitarity implies that the experimental rate for a diffractive Higgs, if and when it will be discovered, is bound to be approximately two orders of magnitude smaller (order of 1%) than the pQCD estimate.

### 6.2 An amplitude analysis of unitarity at very high energies

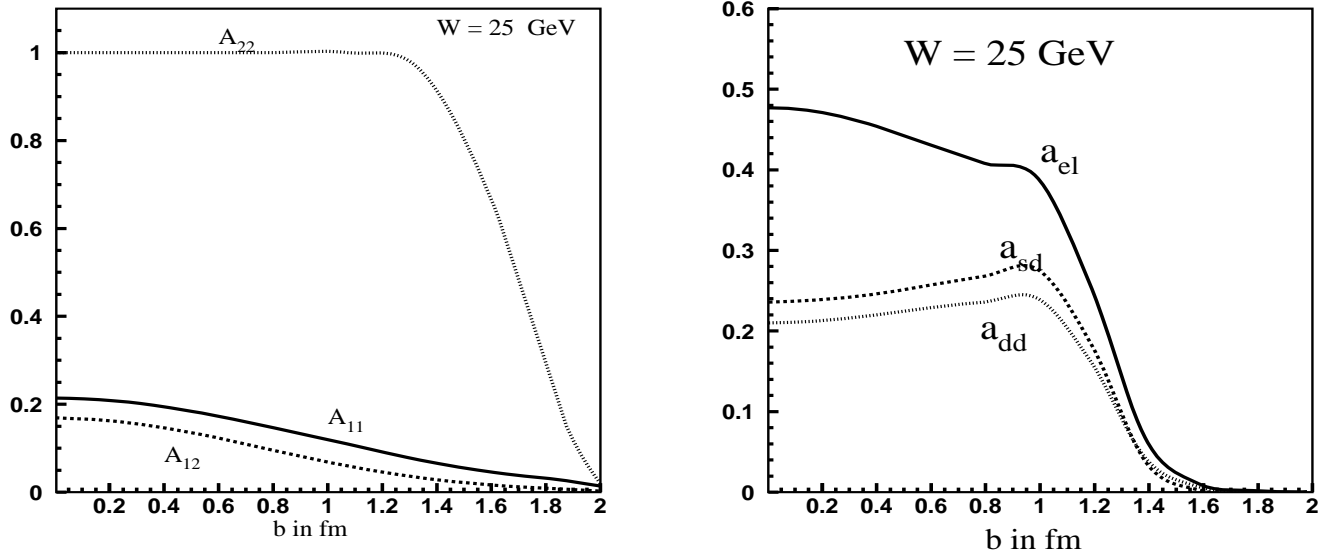


**Figure 9:** Impact parameter dependence of  $A_{i,k}$  and  $a_{el}$ ,  $a_{sd}$ ,  $a_{dd}$  in Model B(2) at  $W = 25 \text{ GeV}$ .

$W = \sqrt{s}$	$a_{el}(b=0)$	$a_{el}$ black core radius fm
TeV		fm
1.8	0.62	
14	0.71	
60	0.79	
250	0.87	
500	0.90	
$10^3$	0.93	
$3 \cdot 10^4$	1.00	0.5
$6 \cdot 10^4$	1.00	0.8
$3 \cdot 10^8$	1.00	2.3
$10^{11}$	1.00	3.0
$1.22 \cdot 10^{19}$ (Planck)	1.00	4.6

**Table 3:** Impact parameter behaviour of  $a_{el}(s, b=0)$ .

The basic amplitudes of the GLM model are  $A_{1,1}$ ,  $A_{1,2}$ , and  $A_{2,2}$  whose  $b$  structure is specified in Eq. (2.5)). These are the building blocks with which we construct  $a_{el}$ ,  $a_{sd}$ ,  $a_{dd}$ , (Eq. (2.11)-Eq. (2.13)). The  $A_{i,k}$  amplitudes are bounded by the black disc unitarity bound. Checking Table 1, it is evident that  $\Omega_{2,2}$  is considerably larger than  $\Omega_{1,1}$  and  $\Omega_{1,2}$ . As a consequence, the amplitude  $A_{2,2}(s, b)$  reaches the unitarity bound of 1 at very low energies. This blackness extends to higher  $b$  values with increasing energy. The observation that  $A_{2,2}(s, b)=1$  at given values of  $(s, b)$  does not imply that the physical elastic scattering amplitude has reached the unitarity bound at these  $(s, b)$  values, see Fig. 9 where we show both the basic amplitudes  $A_{i,k}$ , as well as,  $a_{el}$ ,  $a_{sd}$  and  $a_{dd}$  at  $W=25 \text{ GeV}$ .  $a_{el}(s, b)$  reaches the black disc bound when  $A_{1,1}(s, b)=A_{1,2}(s, b)=A_{2,2}(s, b)=1$ . Accordingly,  $a_{el}(s, b)=1$  and  $a_{sd}(s, b)=a_{dd}(s, b)=0$ . This result is independent of the fitted value of  $\beta$ . A fundamental feature of the GLM models is that  $a_{el}$  approaches the black disc bound at small  $b$  very slowly, reaching it at approximately  $W=30,000 \text{ TeV}$ . See Table 3 and Fig. 10.

A consequence of  $\Omega_{i,k}$  being central in  $b$ , is that  $P_{i,k}^S(s, b)$  is very small at  $b=0$  and monotonically approaches its limiting value of 1, in the high  $b$  limit. As a result, given an input (non screened) diffractive amplitude which is central in  $b$ , the output (screened) diffractive amplitude is peripheral. This important feature, as calculated in Model B(2), is shown in Fig. 11 and Fig. 12 at the Tevatron and LHC energies.

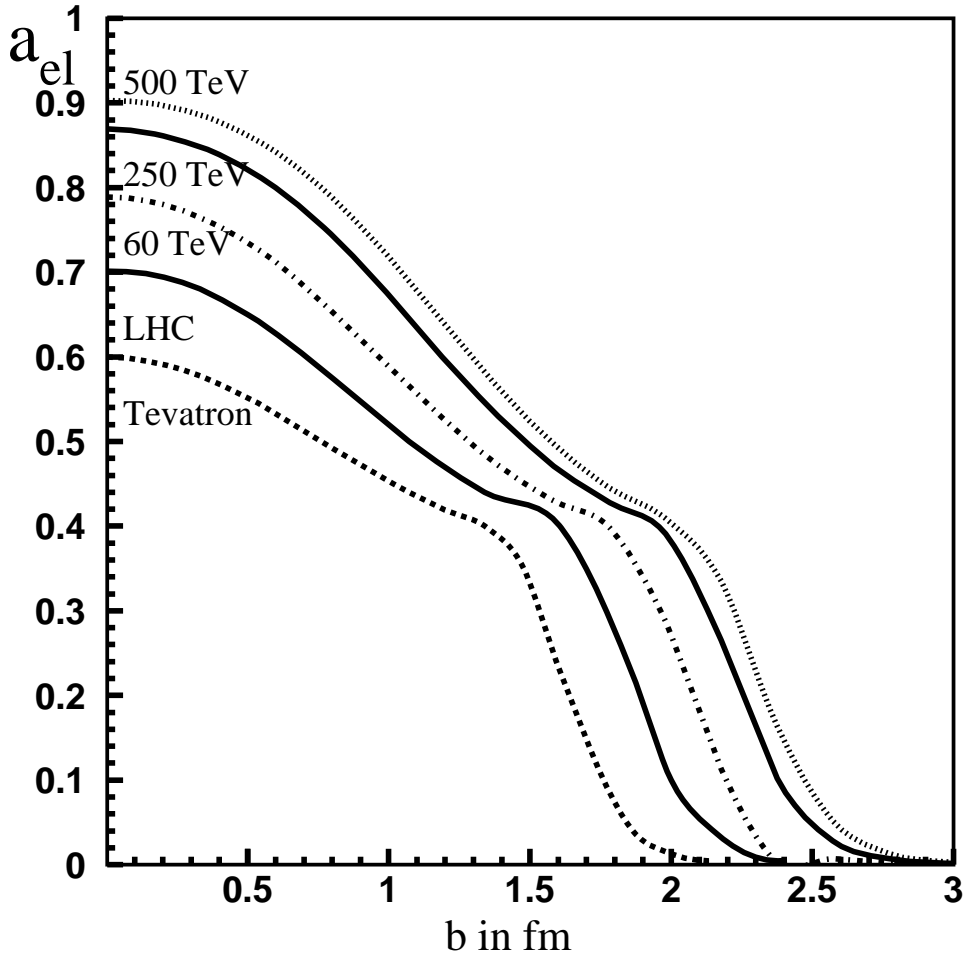


**Figure 10:** Impact parameter dependence of  $a_{el}$  in Model B(2) at different energies.

As expected, the diffractive amplitudes have a local minimum at  $b=0$ , and a maximum at  $b \approx 1.4 fm$  for the Tevatron, which moves to higher values of  $b$  with the growth of energy. This implies a non trivial  $t$  dependence of  $d\sigma_{diff}(M_{diff}^2)/dt$  in the diffractive channels. These qualitative features are induced by Model A, Model B(1) and Model B(2) considered in this paper, even though their detailed behavior, as seen in Fig. 13, are not identical. Experimentally, this feature is not easily tested as it requires a fine grid of  $M_{diff}^2$ .

The implication of the above is that  $A_{2,2}$ , which describes the wave function scattering of  $\Psi_2 \times \Psi_2$ , has (even at  $W$  as low as a few  $GeV$ ) a black central core in  $b$ -space which expands with energy. However, the wave function scattering, corresponding to  $\Psi_1 \times \Psi_1$  and  $\Psi_1 \times \Psi_2$ , are much smaller, well below the black disc bound (see Fig. 11). Consequently, the amplitudes  $A_{1,1}$  and  $A_{1,2}$  have a different behavior as

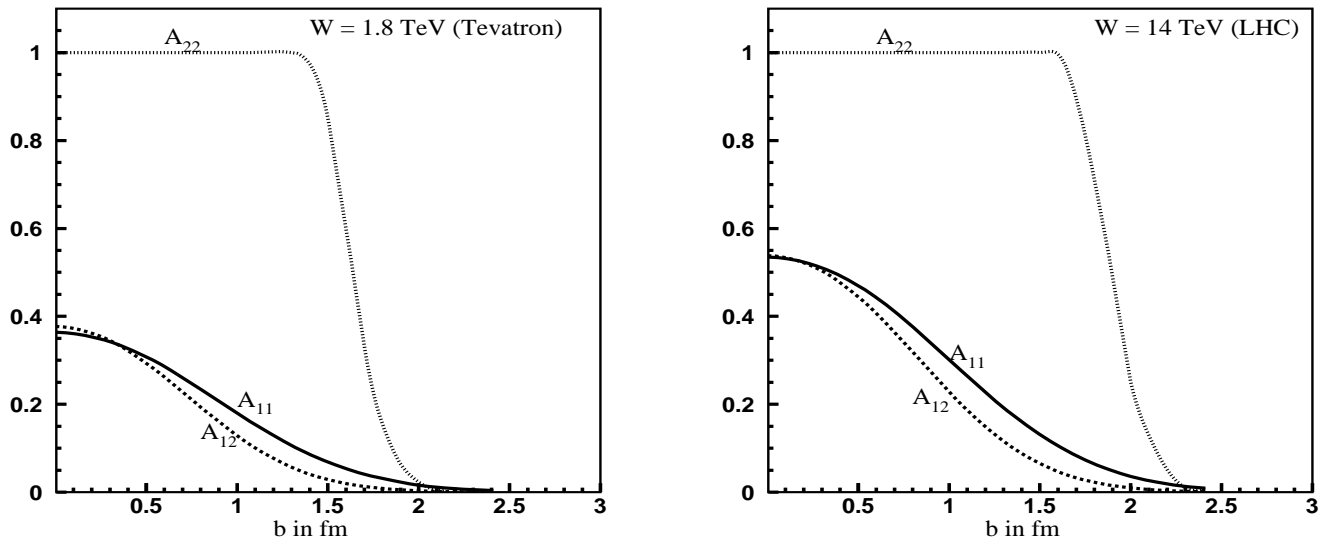


**Figure 11:** Impact parameter dependence of  $A_{i,k}$  at the Tevatron and LHC in Model B(2).

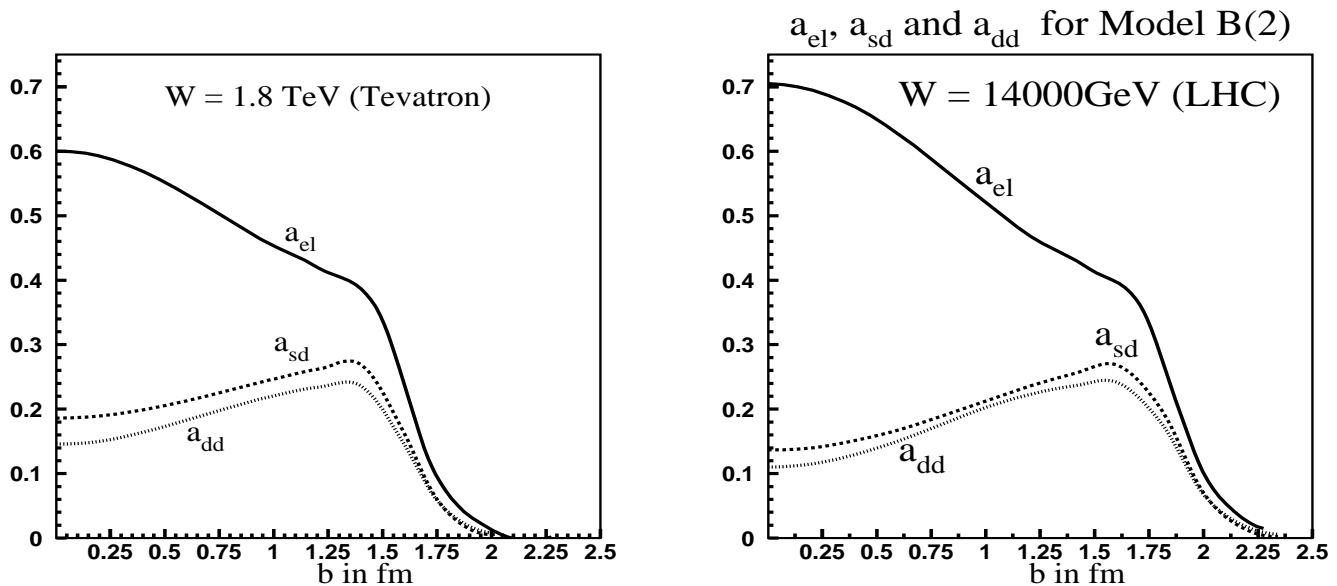


**Figure 12:** Impact parameter dependence of  $a_{el}$ ,  $a_{sd}$  and  $a_{dd}$  at the Tevatron and LHC in Model B(2).

functions of  $(s, b)$ , (see Fig. 11).

The behavior indicated above at the Tevatron and LHC energies becomes more extreme at ultra high energies, when  $a_{el}$  reaches 1 at ever larger  $b$  values (see Table 3). When  $a_{el}(s, b) = 1$ , unitarity implies

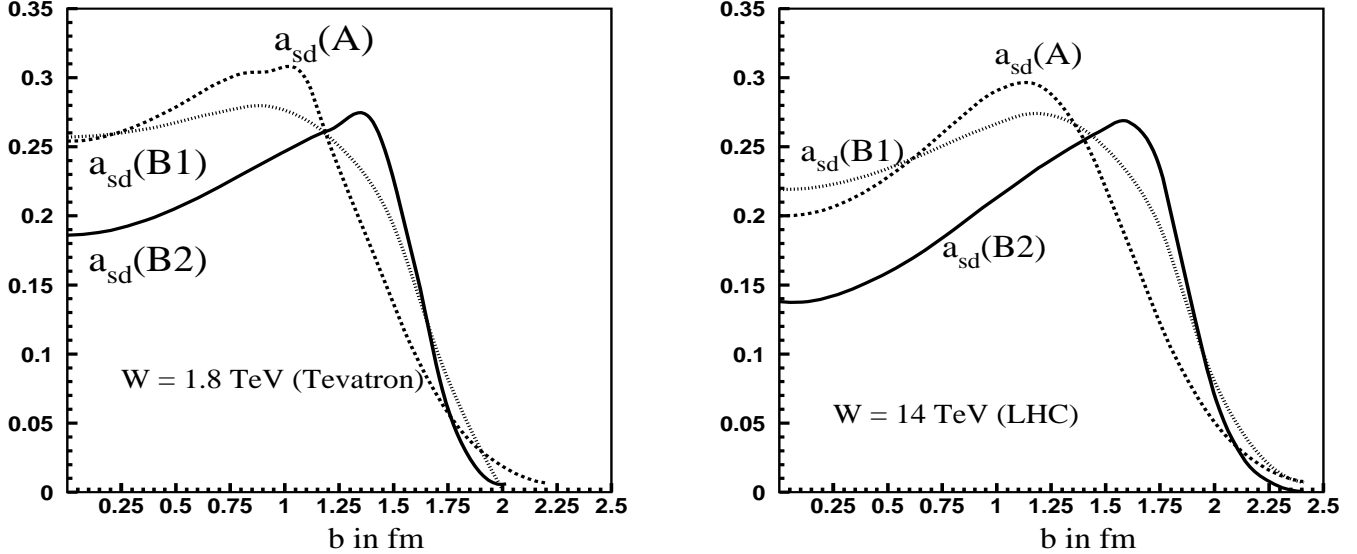


**Figure 13:** Impact parameter dependence of  $a_{sd}$  at the Tevatron and LHC in Models A, B(1) and B(2).

that at these  $b$  values  $a_{sd} = a_{dd} = 0$ . The diffractive cross sections become, thus, highly peripheral and relatively small since they are confined exclusively to the very high  $b$  values where the periphery of  $a_{el}(s, b)$  is below the black disc bound. This prediction is observed in our calculation at ultra high energies, above the GZK ankle cutoff.

We demonstrate this feature and its consequence at the extreme Planck mass. Fig. 14 clearly shows that as the black core of  $a_{el}$  expands, the difference between Models A, B(1) and B(2), considered in this paper, diminishes, being confined to the narrow  $b$  tail where  $a_{el}(s, b) < 1$ . Fig. 15 compares  $a_{el}$ ,  $a_{sd}$  and  $a_{dd}$  in Model B(2). Evidently, the diffractive amplitudes, which are logarithmically suppressed, survive just at the high  $b$  tail of  $a_{el}$ . The above observations may be of interest in the analysis of Cosmic Ray experiments.

## 7. Conclusions

In this paper we have presented a set of predictions for cross sections, forward slopes and survival probabilities at ultra high energies focusing on the LHC. There is a relatively small variance between the published predictions for cross sections at the LHC. Our SD and DD slope predictions are novel and are important for a proper assessment of the soft diffractive background to a diffractively produced Higgs.

We wish to single out three significant properties of our model:

1) We do not assume the existence of a soft Pomeron, and we obtain the best fit with a parametrization which violates Regge (coupling constant) factorization. This feature is in strong contradiction to the elementary features of a soft Pomeron which is defined as a pole in the complex  $J$  plane.

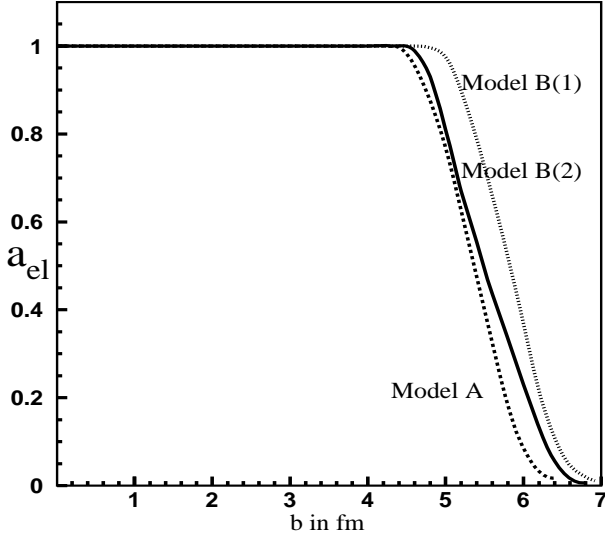


**Figure 14:**  $b$  dependence, at the Planck mass, of  $a_{el}$  in Models A, B(1) and B(2).

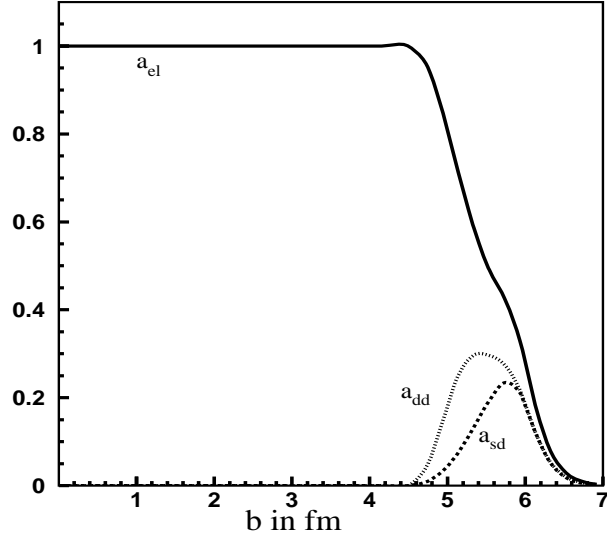


**Figure 15:**  $b$  dependence of  $a_{el}$ ,  $a_{sd}$ ,  $a_{dd}$  at the Planck mass in Model B(2).

- 2) The elastic amplitude is much smaller than unity in the accessible energy range.
- 3) The survival probability for Higgs diffractive production at the LHC is very small,  $S_H^2 = 0.7\%$ .

Our results for the cross sections and the slopes at Cosmic Ray energies up to the GZK ankle are coupled to our analysis of the role of unitarity at high energies. It may appear that our predictions contain two contradicting observations. On the one hand, the centrality in  $b$  space of the output elastic amplitude forces a peripheral  $b$  space behavior on inelastic diffraction [23]. This feature occurs already at low energies, and is reflected in the low values of the predicted survival probabilities, and the consequent suppression of the soft and the hard inelastic diffraction. On the other hand, we obtain a surprising result that the approach of the elastic amplitude to the black disc bound in  $b$  space, is so slow that  $a_{el}$  reaches unity at  $b=0$  only at approximately  $W=30,000 \text{ TeV}$  in the c.m.s. Hence, the elastic amplitude is below the black disc bound all through the measurable Cosmic Ray range. Our result is in sharp contrast to Frankfurt et al. [9] who claim that  $a_{el}$  should reach the black bound already at the LHC.

An intriguing question is how general our results are; i.e. how reliable is our simple parametrization of opacities, and our method of imposing unitarity constraints? The fact that the parameters of our model depend on the parameterization of the Regge sector, introduces some, though small, level of uncertainty. Another weakness is that the GLM model assumes a Gaussian  $b$  dependence of the input amplitudes. This deficiency results in our inability to properly predict the diffractive dip structure and its position in  $d\sigma_{el}/dt$ . As we have seen our model reproduces well [22], the forward cone which contains more than 95% of the data.

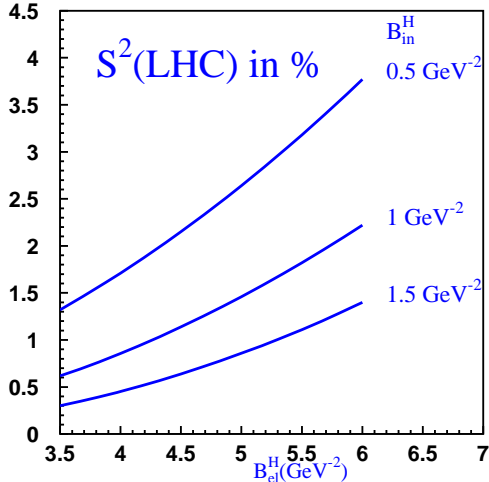


**Figure 16:** The dependence of  $S^2$  at the LHC on  $B_{el}^H$  and  $B_{in}^H$ , the slopes for the hard cross sections.

depend on the values we choose for the elastic and inelastic hard slopes  $B_{el}^H$  and  $B_{in}^H$ . We have determined these parameters from the HERA measured [5, 16]  $J/\Psi$  photo and DIS production elastic and inelastic slopes. Our sensitivity to these parameters is shown in Fig. 16. Note that when we change the value of  $B_{in}^H$  we keep the ratio  $V_{p \rightarrow d}^2/B_{in}^H$  unchanged. Doing so we do not change the cross section of the reaction  $\gamma + p \rightarrow J/\Psi + X$  ( $M \leq 1.6$  GeV).

A possible weak feature of our model is the fact that we possibly do not include Pomeron enhanced diagrams, which in the Pomeron calculus are responsible for high mass diffraction. The CDF collaboration [24] fitting to a triple Pomeron formalism, with  $\alpha_P(0) = 1 + \Delta$ , found that at the Tevatron energy:  $\Delta = 0.112 \pm 0.010(\text{stat}) \pm 0.011(\text{syst})$ . We wish to draw the readers attention to the fact that in the triple Pomeron formalism [19], the diffractive mass distribution is divergent if  $\Delta = 0$ , and it converges for  $\Delta > 0$ . Hence, replacing the rich diffractive final states by the one state, we implicitly assumed that the mass spectrum of diffraction has a typical finite mass. Based on semi-hard processes large mass diffraction has been successfully described in  $e$ - $p$  DIS [4, 5]. We hope to incorporate these processes in our model as well. These semi-hard processes are potentially very important to the calculation of survival probabilities (see Refs. [25, 26]) and can decrease their value further [26].

Regardless of these deficiencies, we believe that a qualitative result similar to ours will be obtained in any model in which the effect of unitarity is significant. These are open problems and should be further pursued. In particular, since we do not have a theory for non-perturbative QCD, the reliability of our calculation should be checked by comparing it with the results obtained for alternate models for soft interactions.

Some additional clarifications concerning our three amplitude Model B(2) prediction of  $S_H^2 = 0.7\%$  are in place. This value is significantly smaller than our two amplitude Model A prediction of  $S_H^2 = 2.7\%$ . We presume that our opacities at small  $b$  do not introduce significant errors in the estimates of  $S_H^2$ . This has been explicitly shown in Ref. [13] for the simple case of a single channel model, where we can assess the  $b$ -profile directly from the  $\frac{d\sigma_{el}}{dt}$  data. For two channel models the  $A_{i,k}$  amplitudes are model dependent and can not be determined directly from the data, hence the resulting  $S_H^2$  is also model dependent. In spite of this, we do have control over the output  $b$ -distribution of  $a_{el}$  which can be compared with the data, very much like the single channel procedure. This is the basis for our intuitive assessment that our estimate of  $S_H^2$  is reasonably reliable, regardless of our choice for the  $b$ -profile. The results we obtain for  $S_H^2$  de-

## Acknowledgments

We are grateful to Eran Naftali, Andrey Kormilitzin and Alex Prygarin for fruitful discussions and technical help. We are indebted to Misha Ryskin with whom we had a most enlightening and beneficial correspondence. UM wishes to thank Daniele Treleani and Mark Strikman for instructive discussions and correspondence. We wish to sincerely thank our anonymous referee whose comments prompted us to improve our presentation. This research was supported in part by the Israel Science Foundation, founded by the Israeli Academy of Science and Humanities, by BSF grant # 20004019 and by a grant from Israel Ministry of Science, Culture and Sport and the Foundation for Basic Research of the Russian Federation.

## References

- [1] E. Gotsman, E. Levin and U. Maor, *Phys. Lett.* **B452**, (1999) 387.
- [2] E. Gotsman, E. Levin and U. Maor, *Phys. Rev.* **D49**, (1994) R4321.
- [3] J. Bartels, E. Gotsman, E. Levin, M. Lublinsky and U. Maor, *Phys. Rev.* **D68** (2003) 054008; *Phys.Lett.* **B556** (2003) 114.
- [4] K. J. Golec-Biernat and M. Wusthoff, *Phys.Rev.* **D59** (1999) 014017; *Phys.Rev.* **D60** (1999) 114023. E. Gotsman, E. Levin, M. Lublinsky, U. Maor, E. Naftali and K. Tuchin, *J. Phys.* **G27** (2001) 2297. J. Bartels, K. J. Golec-Biernat and H. Kowalski, *Phys. Rev.* **D66** (2002) 014001.
- [5] H.Kowalski and D. Teaney, *Phys. Rev.* **D68** (2003) 114005.
- [6] T. Affolder et al., *Phys. Rev. Lett.* **87**, (2001) 141802.
- [7] J. D. Bjorken, *Int. J. Mod. Phys.* **A7**, (1992) 4189; *Phys. Rev.* **D47**, (1993) 101.
- [8] E. Gotsman, E.M. Levin and U. Maor, *Phys. Lett.* **B309**, (1993) 199.
- [9] L. Frankfurt, C. E. Hyde-Wright, M. Strikman and C. Weiss, *Phys. Rev.* **D75**, (2007) 054009; arXiv/0710294[hep-ph]; M. Strikman, private communication to UM.
- [10] K. Goulianos, *J. Phys.* **G26** (2000) 716; *Nucl. Phys. Proc. Suppl.* 99A (2001) 37; *Proceedings of Diffraction 2002, Alushta (Crimea)*, Kluwer Academic Pub. (2002) 13.
- [11] T. Gutman, M.Sc. Thesis, Tel Aviv University (2002).
- [12] E. Gotsman, E. Levin and U. Maor, *Phys. Rev.* **D60** (1999) 094011.
- [13] E. Gotsman, H. Kowalski, E. Levin, U. Maor and A. Prygarin, *Eur. Phys. J.* **C47**, (2006) 655.
- [14] E. Gotsman, E. Levin, U. Maor, E. Naftali and A. Prygarin, "HERA and the LHC - A workshop on the implications of HERA for LHC physics: Proceedings Part A" (2005) 221. (arXiv:hep-ph/0511060[hep-ph]).
- [15] A. Donnachie and P.V. Landshoff, *Nucl. Phys.* **B231**, (1984) 189; *Phys. Lett.* **B296**, (1992) 227; *Zeit. Phys.* **C61**, (1994) 139.
- [16] ZEUS Collaboration, *Nucl. Phys.* **B695** (2004) 3; *Eur. Phys. J.* **C24** (2002) 345.
- [17] M. M. Block, *Czech J. Phys.* **56A** (2006) 77.

- [18] E. Gotsman, E. Levin and U. Maor, *Phys. Lett.* **B438** (1998) 229.
- [19] A. H. Mueller, *Phys. Rev.* **D2**, (1970) 2963; *Phys. Rev.* **D4**, (1971) 150; *Nucl. Phys.* **B415**, (1994) 373; *Nucl. Phys.* **B437**, (1995) 107.
- [20] E. Gotsman, A. Kormilitzin, E. Levin and U. Maor, *Eur. Phys. J.* **C52** (2007) 295.
- [21] V. A. Khoze, A. D. Martin and M. G. Ryskin, *Eur. Phys. J.* **C18** (2000) 167; *Phys. Lett.* **B643** (2006) 93.  
A. B. Kaidalov, V. A. Khoze, A. D. Martin and M. G. Ryskin, *Eur. Phys. J.* **C31** (2003) 387; *Eur. Phys. J.* **C33** (2004) 261.
- [22] M. Ryskin, Private communication containing a calculation of  $\frac{d\sigma_{el}}{dt}$  in our Model B(2).
- [23] G. Cohen-Tannoudji and U. Maor, *Phys. Lett.* **B57** (1975) 253.
- [24] CDF Collaboration, *Phys. Rev.* **D50** (1994) 5535.
- [25] J. Bartels, S. Bondarenko, K. Kutak and L. Motyka, *Phys. Rev.* **D73** (2006) 093004.
- [26] J. S. Miller, arXiv/0610427[hep-ph].

